Journal of Multidisciplinary Engineering Science Studies (JMESS)
ISSN: 2458-925X
Vol. 2 Issue 7, July - 2016

Molarities Concentration Effects Of Some Characterization For (Fe_2O_3) Thin Films Photodetector Applications

Majid H. Hassoni , Noor J. Sahib
Physics Department, Education Faculty,University of Al- Mustansiriyah, Baghdad, Iraq
Corresponding author, E-mail: ahmed_naji_abd@yahoo.com

***Abstract*— In this research study the effect of molarities concentration on the characteristics of films ferric oxide (Fe2O3) which prepared by Chemical Spray pyrolysis (CSP) technique and deposited on silicon substrates used in photodetector is applied to the parameters of the photodetector (short circuit current (Isc) , open circuit voltage (Voc) , (Capacitance –Voltage) characterization (C-V) , spectral responsively (Rλ) , quantum efficiency (η) and minority carrier life time measurement (τLife)).**

The results showed that the photodetector efficiency increasing with increasing molarity concentration of (Fe2O3) films, where the value of the efficiency of the photodetector when the molarity concentration (0.1M) greatest value was of (121%), while the value of the photodetector efficiency when the molarity concentration (0.05M) was (10%).

Keywords—Fe2O3, Photodetectors , AFM, Molarities concentration

1. Introduction

Photodetector are semiconductor devices that can detect optical signals through electronic processes. The extension of wavelength of coherent and incoherent light sources into the far-infrared region on one hand and the ultraviolet region on the other as increased the need for high speed, sensitive photodetector. The photodetector must satisfy stringent requirements such as high sensitivity at operating wavelengths , high response speed , and minimum noise. [1]

The use of semiconducting materials in the form of thin films now a day's occupy prominent place in the basic as well as applied research. It is a technologically useful material due to wide band gap of (2.42 eV) [2] , as many devices such as electronic devices including light emitting diodes, single electron transistors and field effect transistor and sensors [3] . In this research the energy gap which is approach to the value of energy gap in source [2] where the energy gap at concentration (0.05 M) is (2.3eV) , the energy gap at concentration (0.075M) is (2.48eV) and the energy gap at concentration (0.1M) is (2.5eV). Binary oxides M_2O_3 , where M is a trivalent metal, crystallize in the corundum structure and occur in n- as well as p-types [4]. In this category, the hematite (Fe_2O_3) was selected as a prototype due to its technological use as a catalyst [5] . This material is characterized of its good thermal stability at room temperatures, non-toxic, low-cost , numerous, has environmentally friendly properties[6].

2. Experimental

In a model procedure , (0.811, 1.2165 and 1.622) g of ($FeCl_3$), 162.2 g/mol Molar mass (purity 97.0% , Sinopharm Chemical Reagent Co. , Ltd) were dissolved in (100 ml) of distilled water. The solution was added into a round-bottom flask with stirring. The color of the solution was brown. The suspension was kept at 75 °C for (15) minutes. The resultant solution was sprayed on silicon substrates at temperature (375˚C) to get the required thin films.

Crystalline wafer of p-type Silicon with resistivity of (2-20) Ω.cm, 508 μm thickness and (100) orientation were used as starting substrates. The substrates were cut into rectangles with areas of (1×1) cm. After chemical treatment,

(0.1 μm) thick Al layers were deposited by using an evaporation method on the backsides of the wafer. Electrochemical etching then perfect in a mixture (1:1) HF(40%) – Ethanol (99.99) at room temperature by using a (Au) electrode (15 mA/cm^2) Current density

was applied for (fifteen minutes) etching time and the etched area of sample was (0.785 cm2). Silicon substrates lifted from the surface of the heated and cooled after it reaches a temperature to room temperature

Thickness of the samples was measured using the weighting method , by using the relation

$$t = \frac{\Delta W}{\rho \times Area} \quad \ldots\ldots\ldots\ldots\ldots\ldots (1)$$

Where (t) is the thin film thickness , (ΔW) is the change in weight (The difference between the substrate weight before and after the deposition) , (ρ) The density of the thin film material (Fe_2O_3 material density equal to (5.24g /cm^3) and Substrate surface area equal ($1cm^2$). where the use of the thickness of (350 nm) .

3. Results and discussion

(3-1) X-Ray Diffraction:

The results of analysis X-ray diffraction appeared that the thin films of (Fe_2O_3) is multi-crystallizing (Polycrystalline) nature of the type hexagon and the prevailing direction (104), and peaks in the X-ray diffraction diagrams for the films prepared apply and dramatically with the international card (Joint committee on powder diffraction standards) (JCPDS) for (Fe_2O_3) with serial number (00-033-0664).

Table (1) illustrates the portion of the card (JCPDS) and the results obtained from X-ray diffraction of the thin films of (Fe_2O_3) prepared at a temperature (375°C) and three concentrations (0.05,0.075 and 0.1) M

Sample	2θ (degr)	d_{hkl} (Å)	Into. (a.u.)	hkl
(STEM)	24.1378	3.684	22	012
	33.1522	2.7	100	104
	35.6112	2.519	76	110
	54.0892	1.6941	72	116
(0.05 M)	33.1880	2.69724	100	104
	35.6773	2.51455	38	110
(0.075M)	24.1792	3.67788	22	012
	33.1833	2.69761	100	104
	35.6673	2.51523	28	110
	54.1031	1.69374	31	116
(0.1 M)	24.1784	3.678	22	012
	33.1689	2.69875	100	104
	35.6478	2.51656	34	110
	54.0756	1.69454	29	116

The figure (1) exhibit that the intensity of (Fe_2O_3) thin film which deposited from the higher concentration increasing indicated that the crystallization defects.

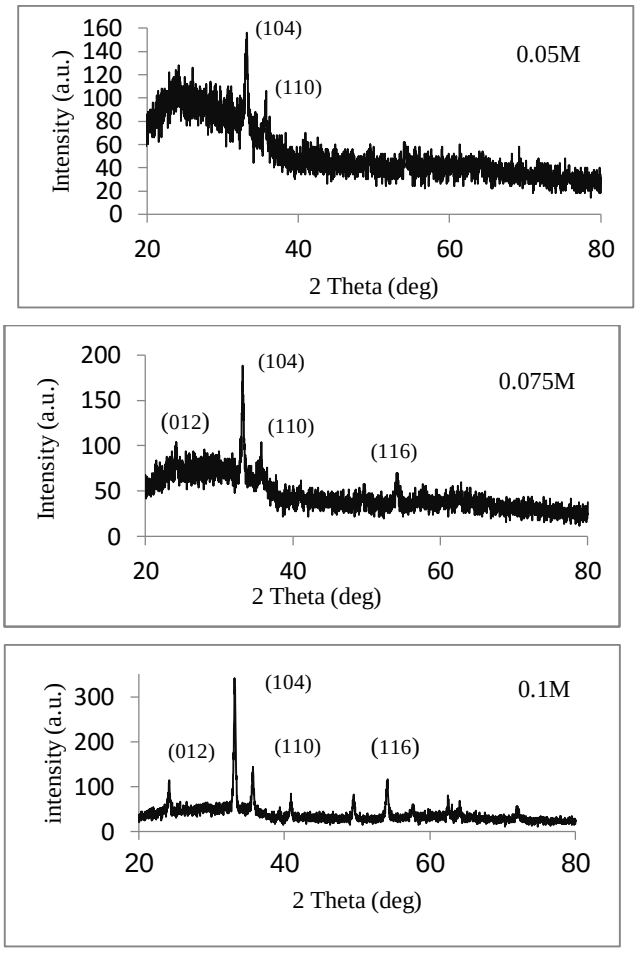

Fig.1: XRD patterns of (Fe_2O_3) thin films prepared by Chemical Spray pyrolysis (CSP) technique and deposited on glass substrate for three concentrations (0.05, 0.075 and 0.1)M.

Crystallite size measurements were determined from the full-width at half maximum (FWHM) of the strongest reflection of the (104) peak, using the Scherer approximation, as in equation (2)

$$G = \frac{K\lambda}{\beta \cos\theta} \qquad (2)$$

Where : (G) the Crystallite size ,

(K) the Scherer's constant it's quantity (0.94) , (λ) the wavelength of the radiation, (β) the full width at half maximum (FWHM) in radians , and

(θ) the Bragg angle.

Table 2: powder X-ray diffraction data (Fe_2O_3) thin film

Samples	Crystallite size (nm)	FWHM (deg)
(0.05 M)	19.0769	0.4167
(0.075 M)	24.89646	0.3193
(0.1 M)	29.48716	0.2696

(2-3)Morphological and Structural Properties of (Fe_2O_3) thin film

Atomic force microscope (AFM) was used as it has the capability to produce micrographs and analyze the surface of the samples under investigation to give very invaluable statistical values of average crystallite size , Roughness average , and the values of the square root of the average square roughness as well as providing us with a lot of important information.

Table (3) shows the values of roughness average, and the values of the square root of the average square roughness, and the average of crystallite size by measuring the atomic force microscope (AFM) to films prepared.

Fe_2O_3 Concentration	Roughness average (nm)	RMS (nm)	Average diameter (nm)
(0.05 M)	4.18	5.08	67.56
(0.075 M)	1.04	1.25	86.83
(0.1 M)	2.42	2.92	107.33

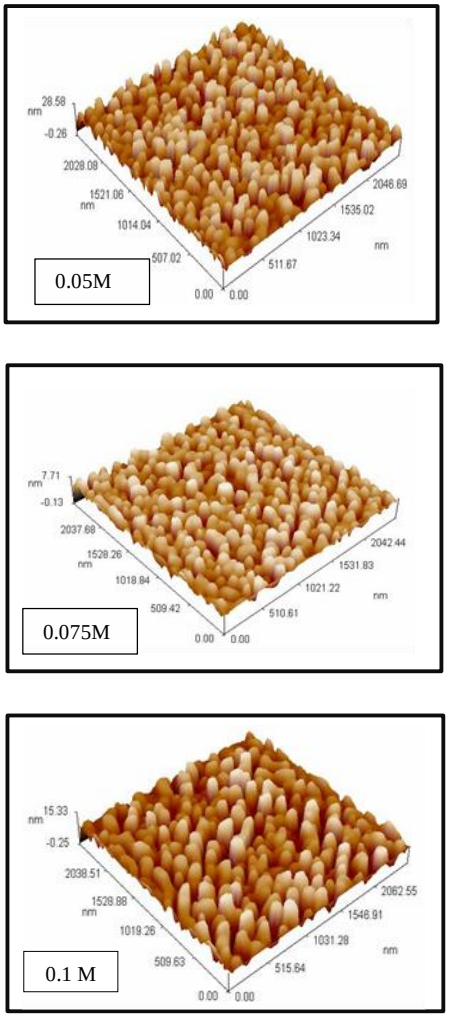

Fig.2: ***AFM images of (Fe_2O_3) thin films as a function of concentration***

(3-3) Optical Properties

The figure (3) shows the transmition as a function the wavelength at a range (350-800) nm, likewise the figure relive that there is no transmittance at the range (350-550) nm. The transmittance started to appear above (550 nm), the increasing in concentration due to decreasing in transmition via that increasing at average grain size.

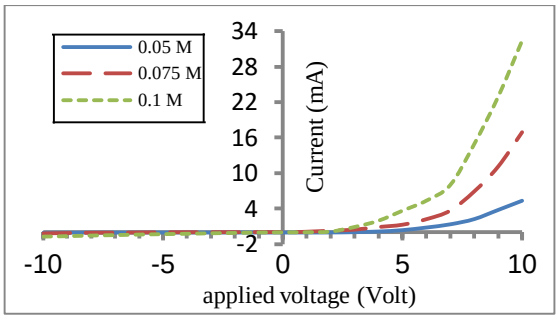

Fig.3: Transmittance spectrum of (Fe_2O_3) thin film which prepared by Chemical Spray pyrolysis (CSP) technique and deposited on glass substrate for three concentration (0.05, 0.075 and 0.1)M

The optical absorption coefficient (α) was evaluated by the relation

$$\alpha h\nu = A(h\nu - E_g)^n \qquad (3)$$

where

$$\alpha = 2.303 \frac{A}{t} \qquad (4)$$

Where (t) is the film thickness and (A) is the absorbency thin film, (hv) is the photon energy, it can be calculated from the relationship

$$E_g = \frac{1240}{\lambda_{(nm)}} \qquad (5)$$

And (n = 0.5) for allowed direct transition. Plotting the graph between $[(\alpha h\nu)^2]$ versus photon energy (hv) gives the value of direct band gap. By drawing a straight line touches the curve even goes a photon energy axis at the point $(\alpha h\nu)^2 = 0$, gives the value of band gap.

Shown in figure (4) the optical band gab is (2.3eV) for concentration (0.0.5M) , (2.48eV) for concentration (0.075M) and (2.5eV) for concentration (0.1M) . This means that whenever the increasing of concentration the value of energy gap increase.

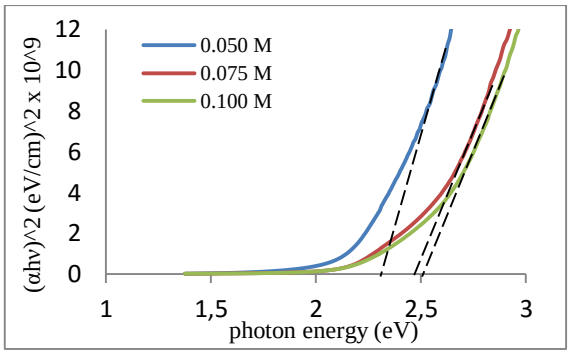

Fig.4: $(\alpha h\nu)^2$ versus photon energy plot of spectrum of (Fe_2O_3) thin film which prepared by Chemical Spray pyrolysis (CSP) technique and deposited on glass substrate for three concentration (0.05 , 0.075 and 0.1)M

(4-3) I-V properties

Figures (5) and (6) shows the (I-V) dark characteristics in forward and reverse direction of solar cells heterojunction divider (p-Si /n- Fe_2O_3) at temperature (375˚C) and thickness (350nm) for three concentrations (0.05, 0.075, 0.1) M. The forward current of photodetector is very small at voltage less than 2 V. This current is known as *(recombination current)* which occurs at low voltages only. It is generated when each electron excited form valence band to conductive band. The second region at high voltage represented the diffusion or bending region which depending on serried resistance. In this region; the bias voltage can transmit electrons with enough energy to infiltrate the barrier between the two sides of the junction.

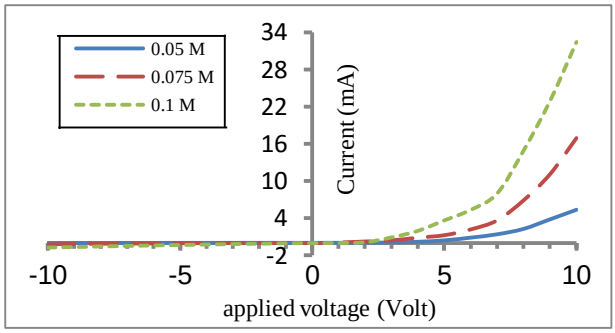

Fig. 5: I-V characteristic under forward reverse bias of the (p-Si /n- Fe_2O_3)

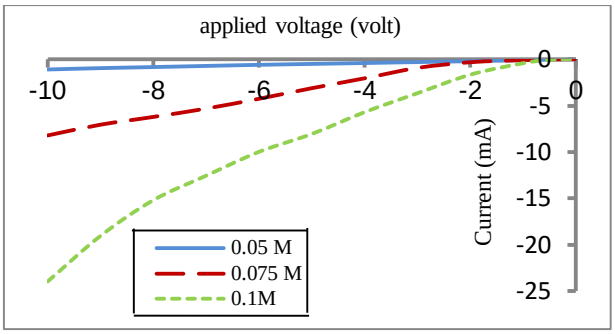

Fig. 6: illuminated (I-V) characteristic of (p-Si /n- Fe_2O_3) photodetector

Figure (6) shows that the reversed current-voltage characteristics of the device measured in dark and the photocurrent under a (41W/m^2) tungsten lamp illumination . Note of figure (6) having two reversed current, the first area is located within the (2.5 Volt) in the status of concentration (0.05M) , (2 Volt) in the status of concentration (0.075M) and (0.7 Volt) in the status of concentration (0.1M) and the resultant from recombination current, while we note that the second region at high voltage represented the diffusion current. The kind of relating current in to both the front and reverse bias voltages it's linear function.

(5-3)(Capacitance –Voltage) Characterization

Figure (7) illustrates the characteristics (capacity - Volt) in the situation of reverse bias at the shed with a range of potential difference (0-6) Volt, where we note that the capacity in a non-linear greater the amount of reverse bias voltage, and as a result of increasing the supply of depletion region (W), an increase voltage reverse

$$C = \frac{dQ}{dV} = \frac{\epsilon_s}{W} \qquad (6)$$

Where (c) is depletion capacity per unit area under reverse bias , (dQ) It represents a partial change in the depletion layer charge per unit area as a result of the change in voltages projector, (W) is showing depletion region ,(ϵ_s) is dielectric constant equivalent to the crossbred junction.

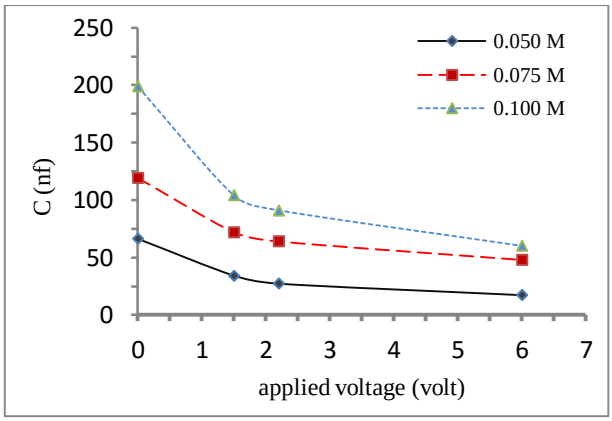

Fig.7: illuminated (C - V) characteristic of (p-Si /n- Fe_2O_3) photodetector

As well as the note from the figure above, the capacity increased with increasing molarity concentration of material used in the preparation for the films.

Figure (8) show that a liner relationship between (C^{-2}) and reverse bias voltage was obtained for the structure.

This linear relationship represented the photodetector two heterojunctions between the (Si / Fe_2O_3) . The values of the built-in potential have been obtained and it has been found (0.5 Volt) for molarity concentration (0.05M) and (1.1 Volt) for both molarity concentration (0.075 and 0.1)M , where we note that the internal construction voltage increases with molarity concentration increases as a result to increase the width of depletion region (W). The internal construction voltage represents the energy required by the electron to transfer from the Si to Fe_2O_3 then from Fe_2O_3 to Si.

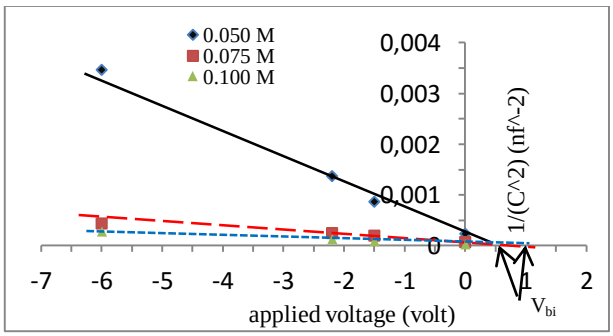

Fig. 8: ($1/C^2$) versus reverse voltage of (p-Si /n- Fe_2O_3) Photodetector for three molarity concentration

(6-3) Spectral Responsively (R_λ)

Figure (9) shows the spectral responsively values (R_λ) as a function of wavelength for three different molarity concentration at a temperature of the substrate (375˚C) and thickness (350nm), where we note that the value of the spectral responsively increased with increasing molarity concentration and we note that the higher the responsiveness of the detector (Fe_2O_3) is (0.8 A / W) in the case of molarity concentration (0.1M) and this may be due to the widening depletion region and to the high absorbance of the film (Fe_2O_3).

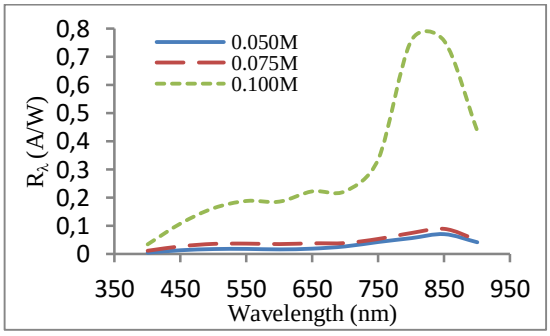

Fig.9: Effect molarity concentration on Spectral Responsively (R_λ)

Table (4) shows the values of responsiveness spectral detector (Si / Fe2O3) for three molarity concentration at a temperature of the substrate (375˚C) and thickness (350nm)

Samples (concentration)	Spectral Responsively (R_λ) (A/W)
0.05M	0.07
0.075M	0.09
0.1M	0.8

(7-3) Quantum Efficiency (η)

This is a measurement of important parameters to determine the efficiency of the performance of the electro-optical devices characterized by the photoelectric effect, such as detectors and solar cells, Where it represents the ratio between the number of charge carriers generated optically to the total number of photons falling on the detector sensitive to light area and this measurement function spectral response (R_λ) and wavelength (λ).

Figure (10) shows the higher the value of the efficiency of the amount obtained when the molarity concentration (0.1M) is (121%) corresponds to the wavelength (825 nm).

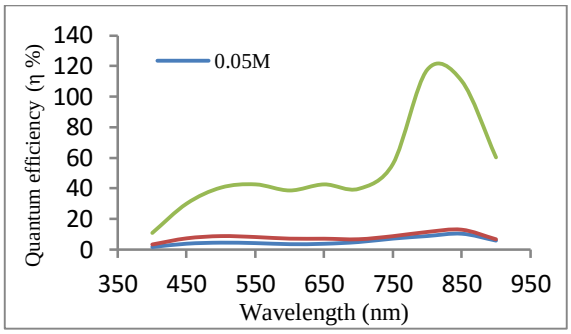

Fig.10: illustrates the efficiency values quantity (η) as a function of wavelength for three different molarity concentration

The reason for this is to characterize, this detector light when the concentration for the rest of the industrialized detectors concentrations of other increased transmittance at this region of wavelengths, leading to increased generation of charge carriers in the depletion between articles similarities area conductive, thereby increasing spectral response (R_λ) which will reflect positively to increase the quantum efficiency (η).[11,12]

Table (5) shows the values of quantum efficiency to detector (Si / Fe2O3) for three molarity concentration at a temperature of the substrate (375˚C) and thickness (350nm

Samples (concentration)	Quantum Efficiency (η %)
0.05M	10
0.075M	13
0.1M	121

(7-4) Minority Carrie Life time measurement

Life time is the average period of time between the time taken to generate carriers process and the process of its reunification [8-13], addition to that determines the efficiency of many semiconductor devices such as photovoltaic solar cells and detectors.

Figure (11) shows that the highest life time has been registered is (2.5 μs) of the detector factory of molarity concentration. The least amount of life time was (5 ms) in the case of molarity concentration
(0.05 M)

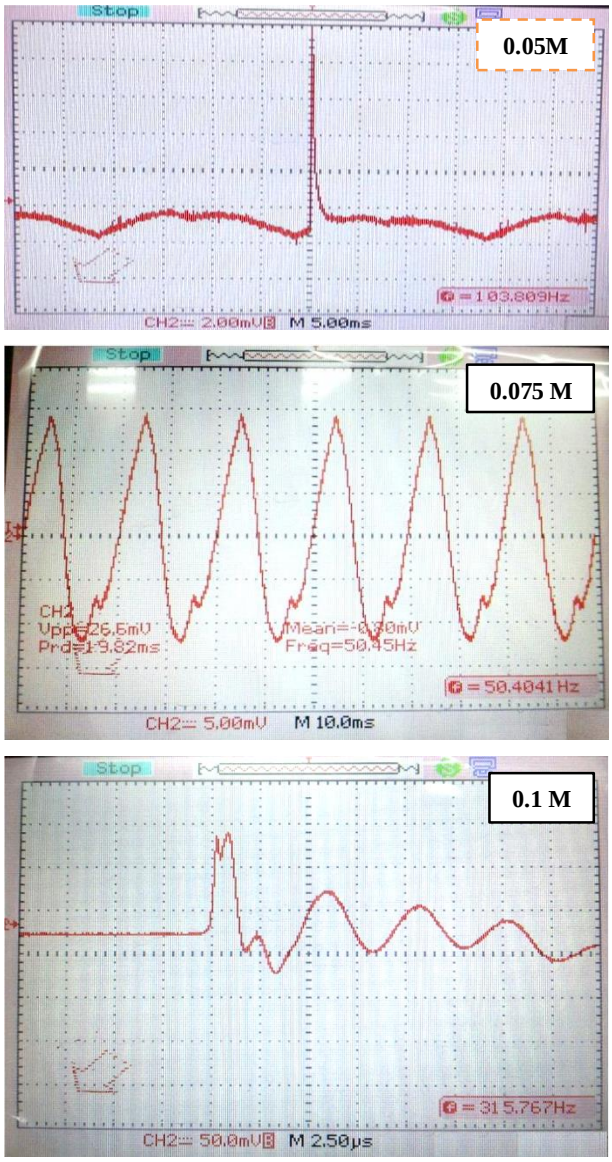

Fig.11: illustrates the life time values for three different molarity concentration

4. Conclusions

Preparation of (Fe2O3) thin films using chemical spray pyrolysis method at different concentration. The results of

X-ray diffraction measurements showed that the thin films of (Fe2O3) prepared at three concentrations (0.05 , 0.075 and 0.1) M were polycrystalline and have hexagonal structure of the type

(□-Fe2O3). The favorite crystal growth for all prepared thin films is (104). The increasing in the concentration of the solution leads to increase in the size of the crystalline grains and improves the crystal structure. The results of the atomic force microscope (AFM) show decrease in the square root of the mean square values of roughness (RMS) when an increase the concentration of the solution. The transmittance started to appear above 550 nm, the increasing in concentration due to decreasing in transmition. Energy gap for direct transmission allowed an increase whenever increase concentration of the solution. The forward current of photodetector is very small at voltage less than (2 V). the reversed current-voltage characteristics of the device measured in dark and the photocurrent under tungsten lamp illumination having two reversed current, the first area is located within the (2.5 Volt) in the status of concentration (0.05M) , (2 Volt) in the status of concentration (0.075M) and (0.7 Volt) in the status of concentration (0.1M) and the resultant from recombination current , While we note that the second region at high voltage represented the diffusion current. The capacity increased with increasing molarity concentration of material used in the preparation for the films. The values of the built-in potential have been obtained and it has been found (0.5 Volt) for molarity concentration (0.05M) and (1.1 Volt) for both molarity concentration (0.075 and 0.1) M . The higher the responsiveness of the detector (Fe_2O_3) is (0.8 A / W) in the case of molarity concentration (0.1M) and this may be due to the widening depletion region and to the high absorbance of the film (Fe_2O_3). The value of the quantum efficiency of the photodetector when the molarity concentration (0.1M) greatest value was of (121%) , while the value of the solar cell efficiency when the molarity concentration (0.05M) was (10%). the highest life time has been registered is (2.5 μs) of the detector factory of molarity concentration. The least amount of life time was (5 ms) in the case of molarity concentration (0.05 M).

References

[1]- S. M. Sze, "Physics of Semiconductor Devices", 3rd Edition. John Wiley and Sons, Canada, (2007).

[2]-Brus L. E. “Electron–electron and electron hole interactions in small semiconductor crystallites: The size dependence of the lowest excited electronic state” J. Chem. Phys. 80, 9 (1984) 4403.

[3]- Dzhafarov T. D., Ongul F., Yuksel S.A.," Effect of indium diffusion on characteristics of CdS films and nCdS/pSi heterojunctions", 84, 2, (2010) 310.

[4] Aroutiounian V M, Arakelyan V M, Shahnazaryan G E,et al. Photoele-ctrochemistry of semiconductor electrodes made of solid solutions in the system Fe_2O_3–Nb2O5. Solar Energy,2006, 80: 1098

[5] Goodenough J B. Metallic oxides. Pergamon Press Ltd, 1971

[6]- M. Allen, D. Willits, J. Mosolf and M. Young, "Protein Cage Constrained Synth-esis of Ferromagnetic Iron Oxide Nano-particles" Adv. Mater, 14, (2002) 1562.

[7]- B. L. Sharma and R. K. Purohit, "Semiconductor Heterojunctions", 1st Edition. Pergamon Press Ltd, NewYork, (1974).

[8]- S. M. Sze, "Physics of Semiconductor Devices", 3rd Edition. John Wiley and Sons, Inc Publication, Canada, (2007).

[9]- J. P. Colinge and C. A. Colinge ,"Physics of Semiconductor Devices", New York , 3rd ed , (2015)

[10]- N. K. Kwok, "Complete guide to Semiconductor Devices", 2nd Edition, Wiley - IEEE Press, U.S.A., (2002).

[11]- A. Rogalski, "Infrared Detectors", 2nd Edition, CRC Press, USA, (2011).

[12]- P. Capper and C. T. Elliott, "Infrared Detectors and Emitters: Materials and Devices", Kluwer Academic Publishers, USA, (2001).

[13]- J. Liu, "Photonic Devices", Cambr-idge University Press, London, (2005).